

Composite electrospun membranes based on PET-PAN modified with LDH-hybrid as promising adsorbent for pollutants removal from wastewater

Abdul Majeed Pirzada ^{1,*}, Imran Ali ^{1,*}, Nabi Bakhsh Mallah ², Ghulamullah Maitlo ³

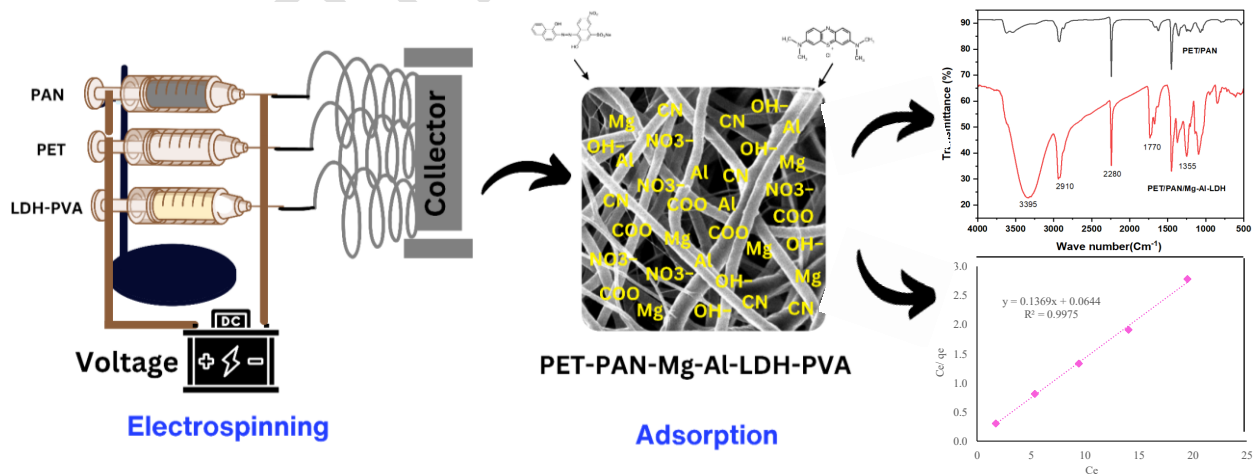
¹ Department of Environmental Sciences, Sindh Madressatul Islam University, Aiwana e Tijarat Road Karachi 74000, Pakistan

² Faculty of Engineering, Science and Technology, Hamdard University, Shahra e Madinat-ul-Hikmat, Karachi 74600, Pakistan

³ Department of Chemical Engineering, Dawood University of Engineering & Technology, New M.A Jinnah Road, Karachi 74800, Pakistan

* Corresponding authors email: ampirzada@smiu.edu.pk ; imran.ali@smiu.edu.pk

Graphical abstract



Abstract

The current work reveals the fabrication of a novel nanofiber composite membrane of PET-PAN modified with Mg-Al-LDH-PVA through electrospinning process. The nanocomposite membranes characterization was conducted with different techniques i.e. SEM, EDS, FTIR, XRD, and water contact angle to evaluate the structure and surface morphology. The optimized nanomembrane was utilized as a useful adsorbent for removal of toxic anionic dye Eriochrome Black T (EBT) and cationic dye Methylene blue (MB) from wastewater. Experimental results identified that PPLP₃ membrane has a potential for the removal of EBT (83%) and MB (52%) at pH 3 and 7, respectively, from aqueous solution. The optimum adsorption capacity of PPLP₃ nanocomposite membrane was identified and calculated as 7.3 mg.g⁻¹ followed by the pseudo 2nd order kinetics and Langmuir adsorption isotherm fit well with R² values of 0.964 and 0.997, respectively. The synthesized nanocomposite membrane could be utilized for effective adsorption of contaminations from different wastewaters.

Keywords: Electrospun membranes; Nanocomposite polymers; Layered double hydroxides; adsorption; dye pollutants.

1. Introduction

Water is regarded as the most important natural resource that is found on this planet. For the survival of any living thing, water is the most required thing. Owing to having a high level of solubility, water is regarded as the universal solvent (Ahmad et al., 2015; Zhang et al., 2016). The key environmental challenge experienced by the people of the world is to maintain the quality of water. As the current level of available reserves of fresh water is insufficient and getting more and more polluted by the passage of time. Such water reserve depletion is causing an inability due to the excess consumption by the increased level of population growth, urbanization,

industrialization, agricultural and other activities (Ayandiran, Fawole, & Dahunsi, 2018; da Silva Alves, Healy, Pinto, Cadaval Jr, & Breslin, 2021; Jeong et al., 2019).

Water contamination is regarded as serious problem worldwide, which has significantly affected the health of people and the life present in the ecosystem (Anandh Babu, Hemavathi, Kousalyadevi, & Shanmuga Priya, 2023; Preethi & Jeyanthi, 2023). Polluted water becomes the main cause of various diseases in the human being which also posed challenges in the field of sciences (Picón, Vergara-Rubio, Estevez-Areco, Cervený, & Goyanes, 2022). The various industries such as cosmetics, plastics, food, textiles, rubber, paper, and printing have released a very large quantity of wastewater which contains the significant amount of toxic indispensable dyes (Khalid, Zubair, & Ihsanullah, 2018; Radoor, Karayil, Parameswaranpillai, & Siengchin, 2020). The untreated wastewater discharge of these dyes into the water bodies give serious threats to aquatic life and human being (Manzar, Waheed, Qazi, Blaisi, & Ullah, 2019). Therefore, introducing new effective methods and materials for removing the pollutants and dyes from wastewater is drastically required (Akram et al., 2023; Bano et al., 2024; Inam et al., 2021; Kishore et al., 2023).

At present, the methods for treating dye wastewater comprise of different categories which include chemical, physical and biological processes. These methods contain several disadvantages, for example they take the high amount of energy along with higher level of costs and produce highly toxic and hazardous byproducts. Therefore, the process of adsorption is regarded as one of the most promising approach because it is easy to operate, less costly and can be recycled with ease and efficient one in comparison with the other conventional techniques (Cheng et al., 2020; Z.-P. Hu, Gao, Liu, & Yuan, 2018).

Electrospinning nanofiber membranes are considered for having capability of dealing with the industrial wastewater, because their structure is highly adjustable along with higher efficiency, porosity, and higher surface area. These attractive characteristics make adsorbents to be prepared using the electrospinning membranes (Dai, Wu, Zhang, Fu, & Li, 2018; Farooqi, Akram, Begum, Wu, & Irfan, 2021; Zhao et al., 2017; Zhu, Zheng, Zhang, & Dai, 2021). At present, many studies are bringing the usage of different homopolymers such as polyethylene terephthalate (PET) and polyacrylonitrile (PAN). In order to prepare the composite membrane modified with the nanoparticles such as layer double hydroxides (LDH) and hybrids of polyvinyl alcohol (PVA) with the purpose of increasing the adsorption removal efficiency for pollutants (Ebrahimi, Nabavi, & Omrani, 2022; Khorram, Mousavi, & Mehranbod, 2017; Mittal, 2021; Sajid, Jillani, Baig, & Alhooshani, 2022).

Previously, many researchers have used different types of polymer combination for fabricating the electrospun nanofibers membrane in order to treat the wastewater. For example, synthesis of different LDHs including MgAl, NiFe and CoAl through co-precipitation technique for the elimination of Eriochrome Black T (EBT) dye and shows adsorption of 540.91 mg.g^{-1} , 132.49 mg.g^{-1} and 419.87 mg.g^{-1} , respectively (Zubair et al., 2017). PVA-Starch modified ZSM-5 zeolite nanomembrane displayed an adsorption for EBT about 2.17 mg.g^{-1} (Radoor et al., 2020). The layered Ag/PDA/PS nanomembrane was fabricated and showed a complete removal of EBT pollutant from effluent (Baig et al., 2022).

The study worked on the fabrication of Fe-SCD-Mg-Al-LDH through ion exchange reaction process and by the method of co precipitation to prepare composite and it display the capability of about 83.40 mg.g^{-1} for color pollutant methylene blue (MB) adsorption (W. Hu, Wu, Jiao, Yang, & Zhou, 2016). PVA-CS modified with nanoparticles CeAlO_3 showed the adsorption for MB about 817.81 mg.g^{-1} (Shahverdi, Barati, & Bayat, 2022). The nanocomposite was fabricated with the help of LDH and activated carbon (AC) through the hydrothermal process. The prepared nanofiber mat showed exceptional attraction for the MB dyes and displayed 250.2 mg.g^{-1} at PH 9. The prepared nanocomposite membrane shown higher efficiency at the room temperature about 816.0 mg.g^{-1} (Aldawsari et al., 2021). PET NF-MWCNTs were prepared and estimated the adsorption for MB about 7.047 mg.g^{-1} (Essa et al., 2022).

Therefore, in this study a new efficient PET-PAN modified using Mg-Al-LDH-PVA was synthesized with electrospun methodology for the removal of EBT and MB color pollutants from effluent. The objective of this research is the utilization of the developed novel membrane as an adsorbent material for the removal of the cationic and anionic dyes i.e. MB and EBT from the effluent. The effect of different operating parameters i.e., pH of solution, adsorption time, pollutant concentration, and membrane dosage were also checked. Adsorption isotherm and kinetics were performed to check the membrane efficiency. The comparison of the current study with other related studies were also performed. Additionally, the proposed adsorption mechanism for pollutant removal was suggested.

2. Methodology

2.1 Chemicals and Materials

In this research, post-consumer waste bottles of PET were used. Likewise, other polymers and chemicals were used in this study, i.e. PVA with an average molecular weight (Mw) of 9,000–10,000 (80% hydrolyzed), white powder form PAN with Mw of 150,000, (Mg(NO₃)₂·6H₂O) magnesium nitrate hexahydrate of 99%, (Al(NO₃)₃·9H₂O) aluminum nitrate nonahydrate ≥ 98%, sodium carbonate powder (Na₂CO₃ ≥ 99.5%), hydrochloric acid (HCl, 37%), sodium hydroxide pellets (NaOH), and sulfuric acid (H₂SO₄), were received from Sigma-Aldrich, Burlington, USA. Also, various other solvents and dyes namely, N, N-Dimethyl formamide (DMF), trifluoro acetic acid (TFA), dichloro methane (DCM), EBT dye, and MB dye were got from Dae-Jung, Busan, South Korea. In addition, the distilled water and analytical research grade type of chemicals were utilized for the research experiments.

2.2 Fabrication of nanoparticles (LDH)

Nanoparticles (Mg-Al-LDH) were synthesized using the coprecipitation method (Alnaqbi, Samson, & Greish, 2020; Qin et al., 2012). During nanoparticle synthesis, as precursors Al(NO₃)₃·9H₂O and Mg(NO₃)₂·6H₂O were used in a proportion of 1:3 (Mg:Al) and under constant pH conditions. 0.025 M of Al(NO₃)₃·9H₂O and 0.075 M of Mg(NO₃)₂·6H₂O of 50 mL mixed aqueous solution and then was added with 50 mL of 0.05 M of Na₂CO₃ and 1 M of NaOH with vigorous and continuous stirring (hotplate magnetic stirrer MS-H280-Pro, OniLab, CA USA). NaOH of 1 M solution was utilized to maintain the solution pH in 9.0-9.5 range. The slurry was aged for 12 h at the set temperature of 65°C. The obtained solid was then processed for centrifuge (80-2 Electronic centrifuge, Atlas medical italiano, China) and cleaned with deionized water several times and kept for drying for 12 h period in an oven (DHG-9202, SANFA, China) at a fixed temperature of 70°C.

2.3 Preparation of electrospinning polymer solution

Polymer solution of PET was prepared by cutting the post-consumer waste PET bottles into square shaped pieces of size $1 \times 1 \text{ cm}^2$ followed by the cleaning and rinsing with deionized water for the electrospinning process. The PET bottle's pieces were then heated in ethanol solution for a duration of 30 min at 40°C to remove the contamination. 5 wt.% homogeneous solution was prepared by dissolving the PET bottle pieces in a DCM-TFA mixture having a ratio of 3:1, followed by mixing at duration of 4 h at room temperature using magnetic stirrer.

Similarly, PAN (8 wt.%) solution in DMF was prepared with continuous stirring for 12 h at ambient temperature. PVA (8 wt.%) solution was prepared in distilled (double) water with continuous stirring for a duration of 5 h at 80°C . Mg-Al-LDH nanoparticles were mixed in PVA (10 gm) solution at different loadings (0.8, 1.2, and 1.6%) for making the Mg-Al-LDH-hybrid solution for PPLP₁, PPLP₂, and PPLP₃ membranes, respectively. Later, the resulting spinnable solution was homogenized by sonicating (Ultrasonic cleaner 2L, China) for 1 h at ambient temperature.

2.4 Fabrication of PET-PAN-LDH-Hybrid membrane

As reported in our previous study, PP and PPLP nanocomposite membranes were synthesized by using electrospinning technique (Pirzada, Ali, Mallah, & Maitlo, 2023). The ready electrospun polymer solutions were transferred into syringes of 10 mL capacity with nozzle diameter of 0.5 mm fitted on top of syringe holders, as illustrated in Figure 1. PP and PPLP nanocomposite membranes were fabricated by co- electrospinning of the polymer solutions at flow rate (0.5 mL.h^{-1}

¹) and speed of drum (30 rpm), DC voltage (19 kV), and 10 cm tip distance. The aluminum covered collecting drum was used for collecting the prepared membranes. The collected membranes were subsequently kept for drying for 24 h at ambient temperature. The prepared nanocomposite membranes were peeled off by employing tweezers for subsequent use in adsorption experiments.

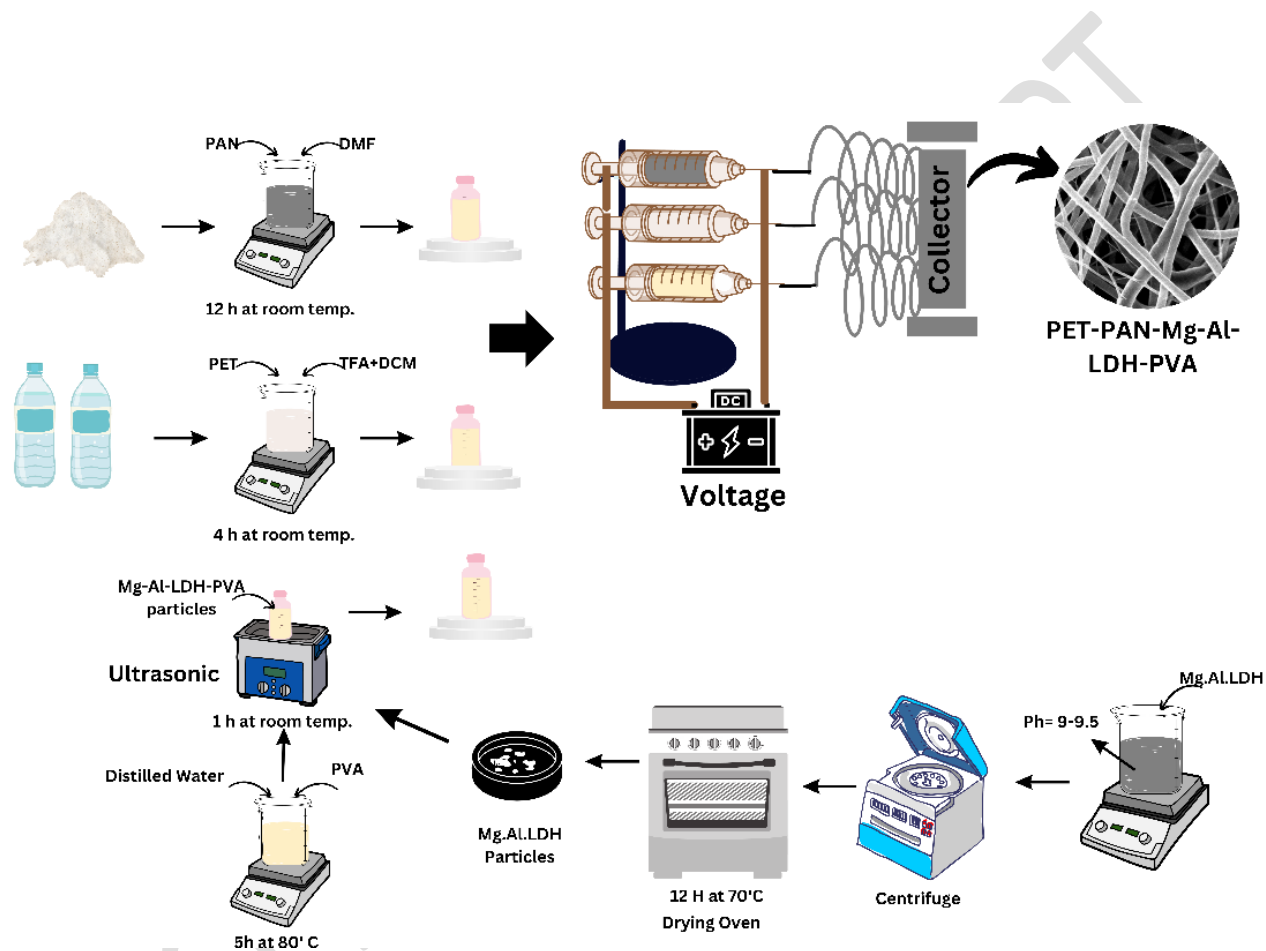


Figure 1. Schematic representation of electrospinning setup for synthesis of PET-PAN-Mg-Al-LDH-PVA nanocomposite membrane.

2.5 Characterization techniques

The physico-chemical properties of the membranes were verified with a variety of techniques. Scanning electron microscopy (SEM, JSM-IT-100, JEOL, Tokyo, Japan) analysis was applied for studying the morphology of the as prepared nanocomposite membrane. To find the average fiber

diameter of electrospun membrane ImageJ software version 1.54-d was utilized for the measurement of 50 fibers diameter distribution. The phase structure and crystal orientation were identified by using Xray diffraction (XRD, D8 Advance, Bruker, Mannheim, Germany). Energy dispersive Xray spectroscopy (EDS, JSM-IT-100, JEOL, Tokyo, Japan) was utilized to analyze membrane's elemental composition. Likewise, infrared spectroscopic analysis of chemical structure and functional groups of membrane was achieved utilizing Fourier Transform Infrared Spectroscopy (FTIR, Perkin Elmer, Waltham, USA) technique. Hydrophilic behavior of the synthesized membrane was determined by water contact angle test.

2.6 Adsorption experiments of EBT and MB

Developed membranes adsorption properties were assessed through basic experiments and were conducted in a 20 mL volume beaker containing EBT and MB aqueous solutions for each set of experiments. Optimization for the assessment of EBT, several parameters were varied one by one like adsorption time 30 ~ 120 min, pollutant concentration 10 ~ 30 mg.L⁻¹, membrane dosage 10 ~ 50 mg and pH 1 ~ 9. A similar method was adopted for the assessment of MB at the optimum parameters, contain pH (7.0), pollutant concentration (10 mg.L⁻¹), membrane dosage (30 mg) and adsorption time (120 min). The solutions pH was maintained with the help of 0.01 M HCL and 0.01 M NaOH. The membranes were taken out from the beakers after the completion of the batch experiments. EBT and MB solutions concentration were estimated by means of UV-Vis spectrophotometer (L7 dual beam, BioBase, Jinan, China) at absorbance wavelength of 530 nm and 665 nm, respectively.

The equations (1 and 2) given below were utilized for measuring the percent of adsorption capacity and removal efficiency of EBT and MB (da Silva et al., 2021; Mansor, Ali, & Abdel-Karim, 2020; Manzar et al., 2019).

$$q_e = \frac{(C_o - C_f)}{m} \times V \quad (1)$$

$$Dye\ Removal(\%) = \frac{(C_o - C_f)}{C_o} \times 100 \quad (2)$$

Here " C_o " stands for the pollutant initial concentration of EBT and MB in $mg.L^{-1}$, while " C_f " is the dye final concentration of EBT and MB in $mg.L^{-1}$, respectively. " q_e " represents the quantity of EBT and MB adsorbed on the surface of membrane in $(mg.g^{-1})$. While " m " represents weight dosage of the adsorbent in (g), and ' V ' denotes the volume in (mL) of pollutant solution.

2.7 Isotherms and Kinetic models

2.7.1 Adsorption Isotherms

Adsorption isotherm models i.e. Langmuir and Freundlich were applied to examine the isotherm of adsorption for the pollutants. As depicted in the model (Langmuir isotherm), the optimum adsorption level is determined by the monolayer adsorption. The surface equilibrium point shows the maximum adsorption in Langmuir isotherm model, and it presented in equation 3 as below (Guo et al., 2021; Habiba, Lee, Joo, Ang, & Afifi, 2019).

$$\frac{C_e}{q_e} = \frac{C_e}{q_m} + \frac{1}{K_L q_m} \quad (3)$$

In this, " C_e " indicates the $\text{mg}\cdot\text{L}^{-1}$ of pollutant concentration equilibrium, " q_e " is the $\text{mg}\cdot\text{g}^{-1}$ of adsorption capacity equilibrium. " K_L " represents the solution affinity, whereas " q_m " is the dye maximum adsorption.

The multilayer process of adsorption for a heterogenous system can be defined by the Freundlich isotherm model. This model can be written as following equation 4 (Pathirana, Dissanayake, Wanasekara, Mahltig, & Nandasiri, 2023).

$$\ln q_e = \ln(k_f) + \ln \frac{C_e}{n} \quad (4)$$

Here, " $1/n$ " indicates the adsorption intensity, and " k_f " is a constant value.

2.7.2 Adsorption Kinetics

The process of adsorption kinetics can calculate the adsorbent's rate of pollutant adsorption. To know the mechanism of adsorption of the membrane, Pseudo-1st- order and 2nd- order kinetics models were utilized. Pseudo-1st- order kinetic adsorption model applies to physical adsorption process, whereas, chemical adsorption relates to pseudo-2nd- order kinetic model (He et al., 2019). The below equations 5 and 6 were used for the kinetic calculations in relation to the pseudo 1st- order and 2nd- order kinetic adsorption models, respectively (Radoor, Karayil, Jayakumar, Parameswaranpillai, & Siengchin, 2021).

$$\log(q_e - q_t) = \log q_e - \frac{k_1}{2.303} t \quad (5)$$

$$\frac{t}{q_t} = \frac{1}{k_2 q_e^2} + \frac{t}{q_e} \quad (6)$$

Whereas " q_t " represents the adsorption capacity in mg/g at time " t ", " q_e " is the mg/g of the adsorbate quantity adsorbed at equilibrium. Whereas " k_1 " and " k_2 " are utilized for the 1st order and 2nd order adsorption rate constant.

3. Results and discussion

3.1 Membrane characterization results

3.1.1 Surface morphology results

The morphology of PP, PPLP₁, PPLP₂, and PPLP₃ membranes surface with different loading of Mg-Al-LDH were investigated by SEM. The morphology image of PP membrane displays the very smooth distribution of nanofibers as shown in Figure 2(a). Similarly, modified nanocomposite membranes PPLP₁, PPLP₂, and PPLP₃ with Mg-Al-LDH-Hybrid revealed the rough and porous structure as compared to the unmodified PP nanomembrane as depicted in Figures 2(b-d), respectively. The synthesized nanoparticles Mg-Al-LDH represent the irregular cubicles and dispersed non uniform porous agglomerates (Abdollahi, Heidari, Mohammadi, Asadi, & Tofighy, 2021; Alnaqbi et al., 2020; Qin et al., 2012). The modified membranes fiber diameter PPLP₁ (623 nm), PPLP₂ (655 nm), and PPLP₃ (671 nm) were achieved to be greater, as compared to the PP (488 nm) as depicted in supplementary information Figure S1(a-d). The increase in fiber diameter of the modified membrane was due to the modification with LDH hybrid. The major factor that influences the enhancement in nanofiber diameter is solution viscosity. The increase in nanofiber diameter with increase in viscosity is discussed in previous studies (Bakhsh, Ahmed, Mahar, &

Khatri, 2021; Habiba, Afifi, Salleh, & Ang, 2017; Nasouri, Shoushtari, & Mojtahedi, 2015; S. Wu, Li, Shi, & Cai, 2022).

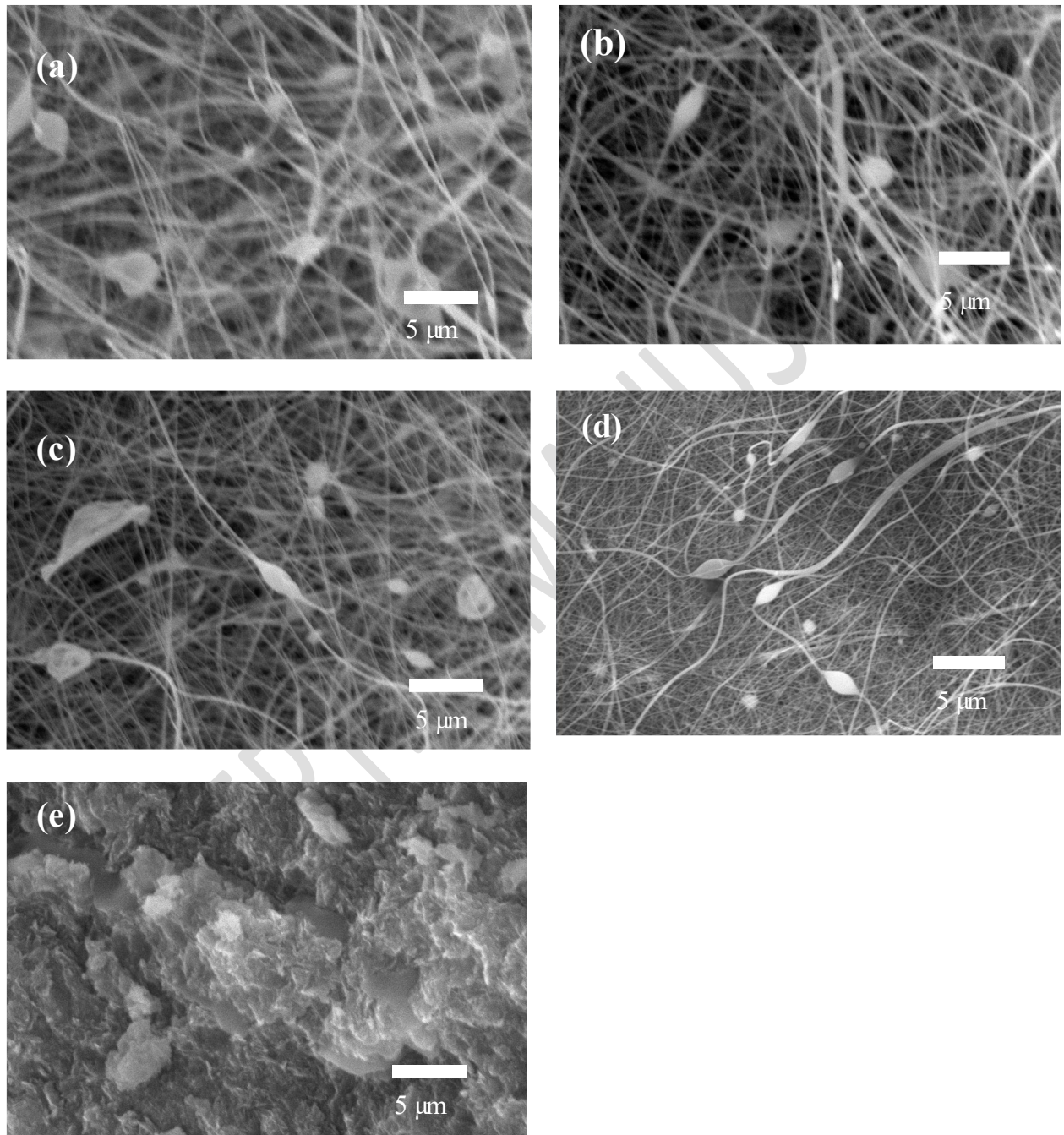


Figure 2. The surface morphology images of: (a) PP, (b) PPLP₁, (c) PPLP₂, (d) PPLP₃ and (e) Mg-Al-LDH nanoparticles.

3.1.2 EDS analysis results

The elemental composition of the modified (PPLP₁, PPLP₂, and PPLP₃) and nonmodified (PP) electrospun membranes and Mg-Al-LDH nanoparticles were identified by using the EDS technique, as depicted in Table 1 and supplementary information Figure S2. The nonmodified PP membrane contains only C, N, and O elements. While modified PPLP membranes contain Mg and Al atoms along with C, N, and O elements. According to Table 1, the elements (Mg and Al) atomic % values were higher (0.25 and 0.63) in PPLP₃ membrane with increasing LDH loading as compared with other membranes. The EDS spectrum displays the occurrence of elements (Mg, Al, O, C, and N) that confirms the successful fabrication of modified membrane.

Table 1. EDS elemental composition (atomic %) of PP, PPLP₁, PPLP₂, PPLP₃, and Mg-Al-LDH.

| Sr # | Type | Mg | Al | C | N | O |
|------|-------------------|-------|------|-------|------|-------|
| 1 | LDH | 15.11 | 5.30 | 11.93 | - | 67.40 |
| 2 | PP | - | - | 89.49 | 5.14 | 5.37 |
| 3 | PPLP ₁ | 0.21 | 0.19 | 62.46 | 5.81 | 31.33 |
| 4 | PPLP ₂ | 0.37 | 0.24 | 55.79 | 5.37 | 38.23 |
| 5 | PPLP ₃ | 0.63 | 0.25 | 60.02 | 6.45 | 32.65 |

3.1.3 FTIR results

Figure 3(a) represents the functional groups characterization of modified (PPLP₃) and unmodified (PP) membranes were analyzed by FTIR technique. PAN nanofibers spectra presented the characteristic peaks due to stretching vibration of -CH₂- occurred at 1455 cm⁻¹ and 1073 cm⁻¹.

The stretching bands of nitrile group $-\text{C}\equiv\text{N}$ of PAN nanofibers revealed the characteristics peak at 2280 cm^{-1} (Hartati et al., 2022; Shakiba, Abdouss, Mazinani, & Kalae, 2023; Xu et al., 2022). The PET peaks were occurred at 2910 cm^{-1} and 1770 cm^{-1} representing to be formed by methylene groups ($-\text{CH}_2-$) longitudinal and oscillation of carbonyl ($\text{C}=\text{O}$) group, respectively (Khorram et al., 2017). The PVA spectrum, resonance band were appeared at 3395 cm^{-1} due to the presence of the $-\text{OH}$ group and characteristics band of $\text{C}-\text{H}$ group was observed at 2909 cm^{-1} (S. Wu et al., 2022). The developed Mg-Al-LDH nanoparticles spectrum band at 3395 cm^{-1} , were due to the existence of hydroxyl (OH) vibration stretching. Peaks at 1355 cm^{-1} and 1670 cm^{-1} occurred by the presence of NO_3^- (Novillo et al., 2014). The characteristics bands confirm the fabrication of modified and unmodified membranes.

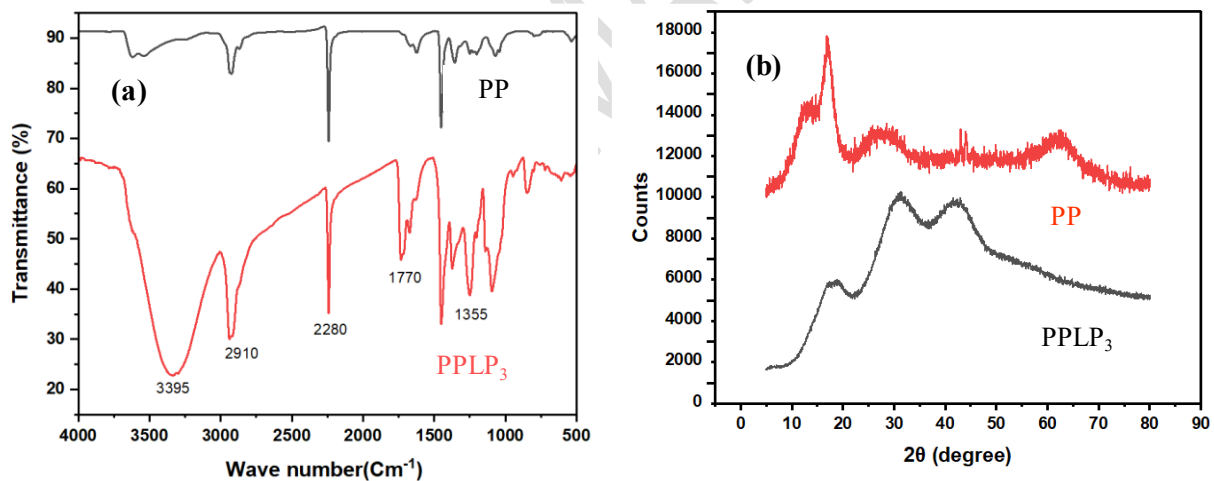


Figure 3. PP and PPLP₃ membranes: (a) FTIR spectrum and (b) XRD analysis.

3.1.4 XRD results

Figure 3(b) displayed the XRD analysis of PP and PPLP₃ membranes. The XRD pattern observed for PET displayed peak at $2\theta = 17^\circ$ (Aziz et al., 2021; Q. Wang, Geng, Lu, & Zhang, 2015; Yasin,

Sharaf Zeebaree, Sharaf Zeebaree, Haji Zebari, & Saeed, 2021). Whereas three sharp diffraction peaks of PAN were identified at $2\theta = 18^\circ$, 22° , and 26° that represent to the crystalline structure (Chiu, Lin, Cheng, & Chou, 2011; Makarov et al., 2022; Ullah et al., 2019). Furthermore, major sharp peaks of Mg-Al-LDH nanoparticles were occurred at $2\theta = 31^\circ$ and 44° (Alnaqbi et al., 2020; Swain, Barik, Pradhan, & Behera, 2018). The XRD pattern for PVA was observed at peak $2\theta = 19.5^\circ$ (Qin et al., 2012). The result of XRD analysis of PET, PAN, LDH and PVA showed the successful synthesis of PPLP membrane.

3.1.5 Hydrophilicity measurement

The wettability performance of PP and PPLP₃ nanocomposite membranes was measured by water contact angle technique. As shown in Figure 4, the water contact angle of PPLP₃ membrane (19°) is lower than the PP membrane (81°). The reduction in contact angle values of PPLP₃ electrospun membrane showed better hydrophilicity properties as compared to the PP membrane. Increased in membrane hydrophilicity may be due to the cause of surface roughness (Jiang, Zhao, & Zhai, 2004; X. Li, Ding, Lin, Yu, & Sun, 2009; Skorniyakov & Komar, 1998; N. Wang, Zhao, & Jiang, 2008). The wettability of the PPLP₃ membrane increased may also be due to the addition of LDH-hybrid (Jia, Liang, & Yang, 2021; G. Li, Zhao, Lv, Shi, & Cao, 2013). The decrease in water contact angle will help to enhance the adsorption of pollutant removal from wastewater.

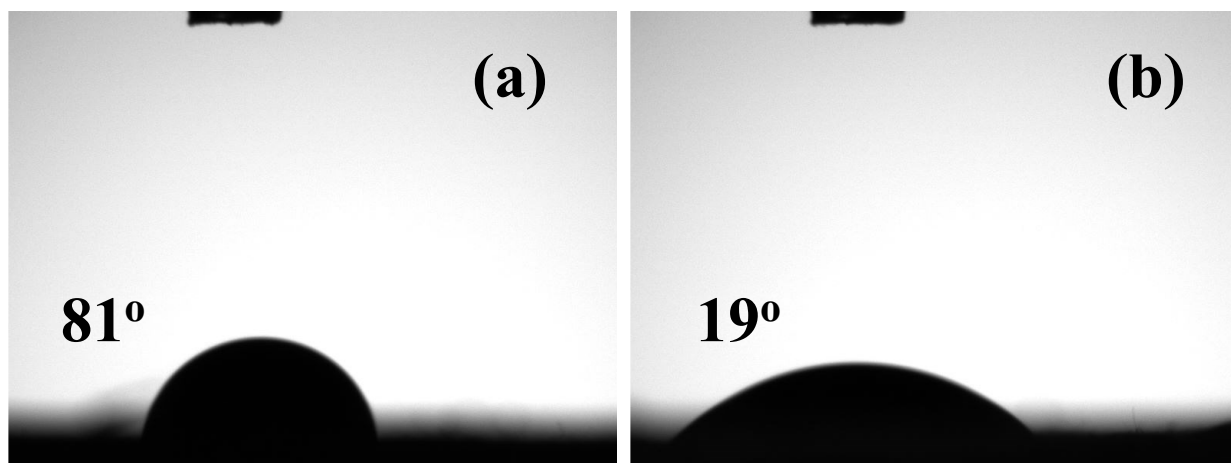


Figure 4. Hydrophilicity analysis using water contact angle test: (a) PP and (b) PPLP₃ membranes.

3.2 Initial adsorption experiment results

Firstly, basic experiments were achieved to examine the adsorption efficiency of the modified PPLP₁, PPLP₂, and PPLP₃ membranes and nonmodified PP membranes for EBT and MB dyes. PPLP₃ membrane removal efficiency for pollutants EBT (83%) and MB (52%) is higher than that of other membranes as shown in supplementary information Figure S3. The increased removal efficiency of pollutants occurred through the surface phenomena, wettability, and the existence of the functional groups on the surface of membrane (C–N, C–O, –OH, etc.). The PPLP₃ membrane was used to perform additional experiment trials for kinetic and adsorption isotherm models. The parameters to check the adsorption efficiency of MB and EBT are shown in supplementary information Table S1.

3.3 Optimization of adsorption experiment

3.3.1 pH

A solution's pH significantly affects the adsorption process as it influences both efficiency and behavior of adsorption method. The minor variation in the solution's initial pH could affect the

removal efficiency, while it also influencing the solution's properties and the membrane surface charge (Anah & Astrini, 2017). The experimental design for the assessment of EBT adsorption on the surface of membrane was performed with the variation in pH 1 ~ 9 keeping initial pollutant concentration (10 mg.L⁻¹), adsorption time (90 min), and membrane dose (30 mg). It was observed that at pH 3 the EBT adsorption shows maximum removal efficiency 83% as presented in Figure 5(a). From the experimental results it was identified that when the solution pH was increased, the removal efficiency of EBT decreases. At pH 3, maximum adsorption performance obtained may be associated to the surface characteristics of the electrospun membrane (Radoor et al., 2021; Xu et al., 2022).

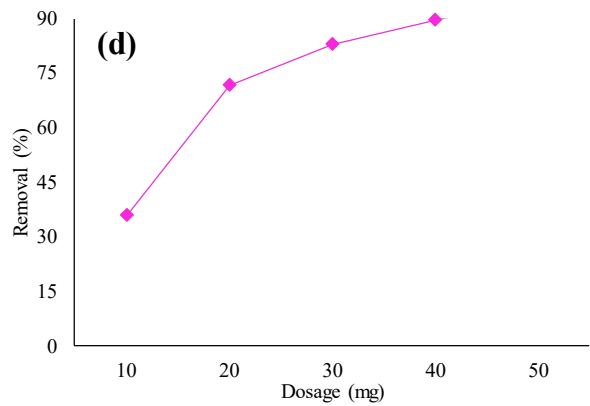
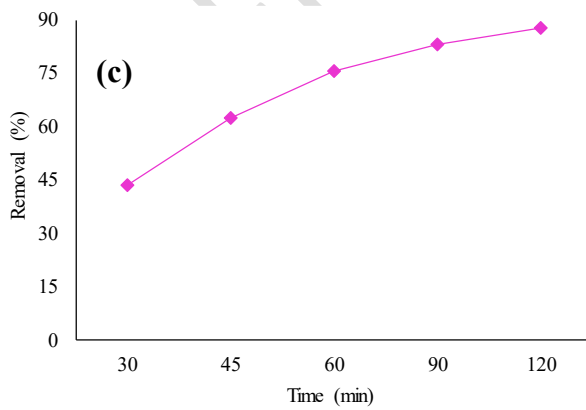
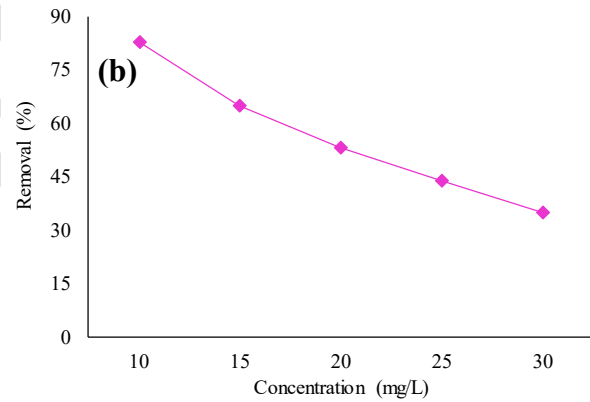
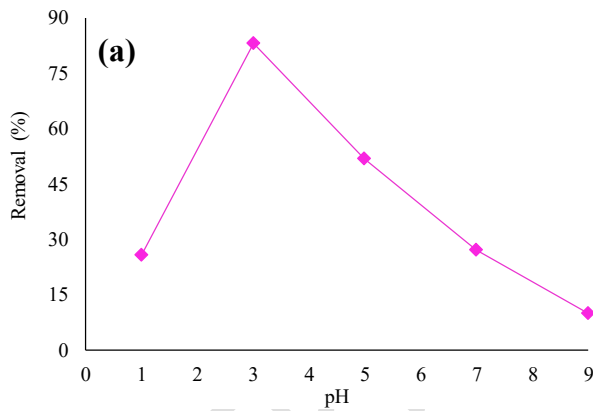


Figure 5. Effect of: (a) solution pH, (b) pollutant concentration, (c) adsorption time, and (d) membrane dosage on EBT removal using PPLP₃ membrane.

3.3.2 Initial dye concentration

In order to examine impact on the adsorption of EBT, the pollutant concentration was adjusted in between 10 to 30 mg.L⁻¹. With the gradual rise in the pollutant concentration, there was a drop in the efficacy of EBT adsorption; Figure 5(b) shows that the optimum removal performance of EBT was at 10 mg.L⁻¹. Higher pollutant concentration leads to decrease in percentage of dye elimination at the same adsorption time (Khan et al., 2021; Y. Wu et al., 2013).

3.3.3 Contact time

Several tests were carried out to obtain maximum equilibrium time that tends to offer the optimum EBT adsorption. The adsorption efficiency of EBT at varying contact times (30 ~ 120 min) are shown in Figure 5(c). Because of the existence of adsorption functional groups and active sites on the PPLP₃ membrane surface, the adsorption efficiency values for EBT increased initially. Later, a gradual trend was noticed till it achieves equilibrium condition which was attained after 90 min. It has been noted that the active sites on the membrane surface of every polymer has a separate equilibrium duration due to the active functional groups (Chaukura, Murimba, & Gwenzi, 2017; Y. Wu et al., 2013).

3.3.4 Membrane dosage

The dosage of the adsorbent is also one of the significant factors that influence the membrane materials adsorption efficiency. Varying in the adsorbent dosage of PPLP₃ from 10 ~ 50 mg the

efficiency of the removal of EBT was analyzed. It was observed that the increase in the membrane dosage results in an improved pollutant adsorption by the membrane (Bensalah, Younssi, Ouammou, Gurlo, & Bekheet, 2020). Therefore, the result shows the enhanced adsorption process is due to the increase of active adsorption sites on the PPLP₃ membrane surface, which is because of the increase in membrane dosage (Eltaweil, Mohamed, Abd El-Monaem, & El-Subruiti, 2020). As shown in Figure 5(d), the maximum 95.4% of EBT removal was achieved with a PPLP₃ dosage of 50 mg. For further experiments the optimum PPLP₃ dosage was selected as 30 mg.

3.4 Adsorption Isotherms

The isotherms models i.e. Freundlich and Langmuir were utilized to explore the PPLP₃ membrane's adsorption capacity. An adsorption isotherm analysis was achieved to identify the functions of the membrane quantity attached to the membrane's surface (Al-Sou'od, 2012). Figure 6(a-b) and Table 2 present a relationship of the adsorption parameters derived from the Freundlich and Langmuir isotherms model for the adsorption of EBT on PPLP₃ nanomembrane surface. For dye adsorption on PPLP₃ the Langmuir isotherm was observed suitable with R² value of 0.997. According to Table 2, the Langmuir isotherm model was observed to be sufficiently applied to the membrane adsorption process and is suitable to PPLP₃ membrane having an optimum EBT adsorption capacity of 7.3 mg.g⁻¹.

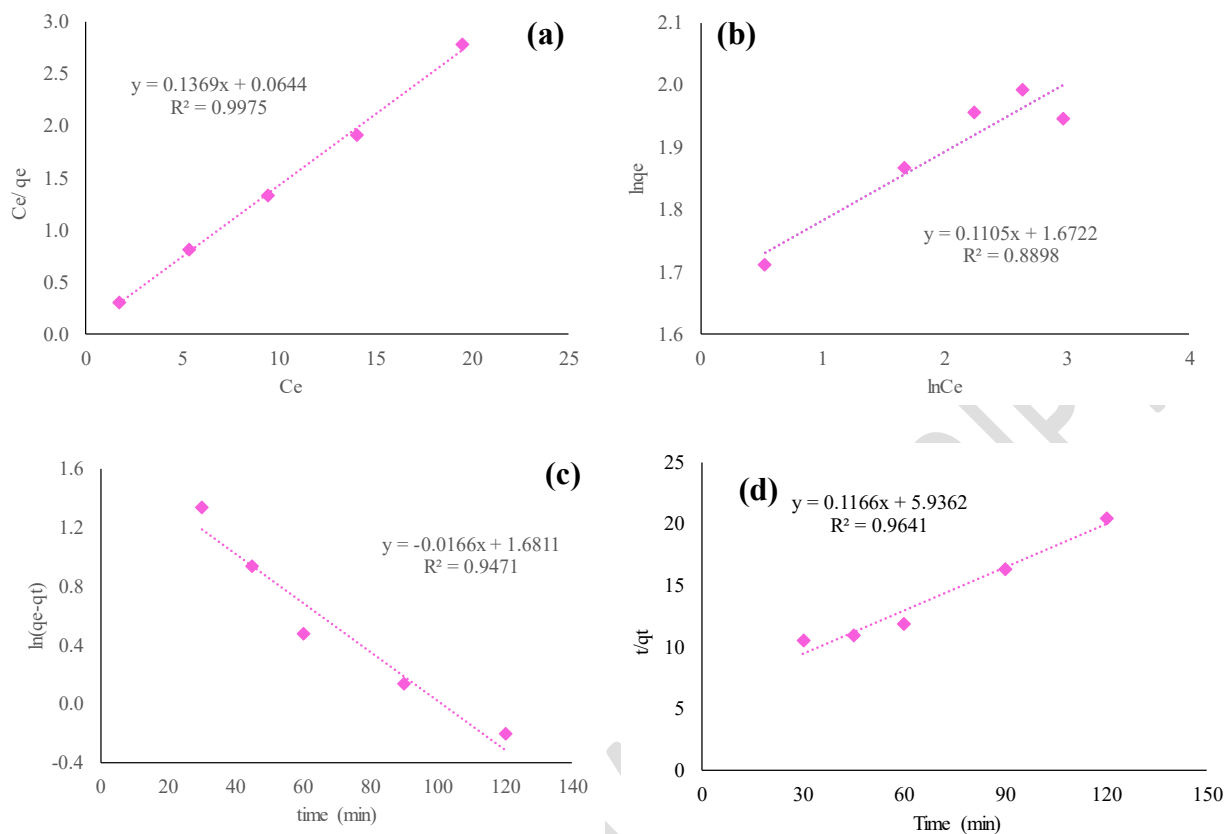


Figure 6. Adsorption isotherm models for EBT: (a) Langmuir and (b) Freundlich. Adsorption kinetic curves of EBT: (c) pseudo-1st order and (d) pseudo-2nd order.

Table 2. Parameters for Langmuir and Freundlich adsorption models, pseudo-1st order and pseudo-2nd order kinetic models.

| Langmuir Isotherm | | | Freundlich isotherm | | |
|----------------------------------------------|-----------------------------------------|-------|-----------------------------------------------------------------------------------|-------|-------|
| q_{\max} ($\text{mg}\cdot\text{g}^{-1}$) | K_L ($\text{L}\cdot\text{mg}^{-1}$) | R^2 | K_F ($\text{mg}\cdot\text{g}^{-1}$)($\text{L}\cdot\text{mg}^{-1}$) $^{1/n}$ | $1/n$ | R^2 |
| 7.3 | 2.126 | 0.997 | 5.3 | 0.1 | 0.889 |
| Pseudo-1 st order | | | Pseudo-2 nd order | | |

| q_e (mg.g ⁻¹) | k_1 (1/h) | R^2 | q_e (mg.g ⁻¹) | k_2 (g.mg ⁻¹ .h ⁻¹) | R^2 |
|-----------------------------|-------------|-------|-----------------------------|----------------------------------------------|-------|
| 5.37 | 0.017 | 0.947 | 8.58 | 0.002 | 0.964 |

3.5 Adsorption Kinetics

The obtained experimental data were fitted into various kinetic models to examine the adsorption mechanism and adsorption rate constant. As shown in Table 2 and Fig. 6(c-d), the pseudo-1st and pseudo-2nd order model parameters were identified, and the corresponding R^2 values were found to be 0.947 and 0.964, respectively. The pseudo-2nd order model gives a well explanation of the EBT adsorption mechanism as compared to the pseudo-1st order model. The pseudo-2nd order model is fit well in the current research, as it is effective at managing the EBT adsorption onto the PPLP₃ membrane surface. This also provided that the adsorption mechanism is done through the process of chemisorption process (Konicki, Aleksandrak, Moszyński, & Mijowska, 2017; L. Li, Luo, Li, Duan, & Wang, 2014).

3.6 Proposed PPLP adsorption mechanism

The adsorption mechanism is primarily caused by ions or liquid molecules adhering on the PPLP membrane surface. It happens because of the reason of force of attraction in between the adsorbent and adsorbate (Konicki et al., 2017; L. Li et al., 2014). Figure 7 discusses the suggested mechanism process of adsorption in between EBT, MB and the PPLP membrane. It was evident from characterization results that there are different functional groups present in the PPLP membrane. Due to electrostatic force of attraction or hydrogen bond, the dye EBT having N=O functional group is adsorbed on the PPLP membrane (Dhar et al., 2022; Zubair et al., 2017). Similarly, hydroxyl ions on the PPLP membrane is most likely to participate in MB adsorption through

electrostatic force of attraction (Dhar et al., 2021; Pan et al., 2020). Table 3 displays the comparison performance of PPLH₃ membrane with other related studies, which shows that this membrane can remove pollutants efficiently.

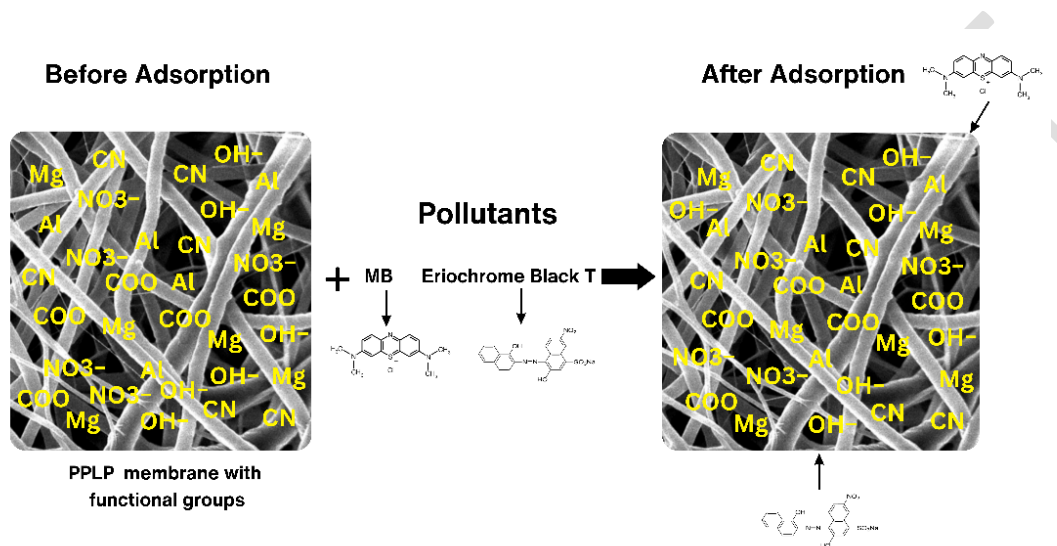


Figure 7. Proposed adsorption mechanism of MB and EBT dyes for PPLP membrane.

Table 3. Summary of comparative studies of the current research with others related research.

| Sr No. | Adsorbent type | Target pollutant | Solution pH | Adsorption time (min) | q_{\max} (mg.g ⁻¹) | Reference |
|--------|----------------------------------------|------------------|-------------|-----------------------|----------------------------------|-----------------------|
| 1 | PET-PAN-Mg-Al-LDH-PVA | EBT | 3 | 90 | 7.30 | This study |
| 2 | Polyvinyl Alcohol/Starch/ZSM-5 Zeolite | EBT | 3 | 180 | 2.17 | (Radoor et al., 2020) |

| | | | | | | |
|---|-----------------------------------------------------|-----|----|-----|-------|----------------------------------------------|
| 3 | CTAB-PA | EBT | 4 | -- | 89.93 | (Ben Arfi, Karoui, Mougine, & Ghorbal, 2019) |
| 4 | PET NF-MWCNTs | MB | 8 | 120 | 7.05 | (Essa et al., 2022) |
| 5 | OMWCNT-K-Carrageenan-Fe ₃ O ₄ | MB | -- | 360 | 1.24 | (Duman, Tunç, Polat, & Bozoğlan, 2016) |

4. Conclusions

The nanocomposite membrane was successfully synthesized using PET-PAN modified with Mg-Al-LDH hybrid with the electrospinning technique, and was confirmed by SEM, EDS, FTIR, and XRD results. From SEM results it was observed that the membrane diameter was increased with addition of LDH hybrid. The addition of different concentration of Mg-Al-LDH, the PPLP membrane's hydrophilicity was improved with notable adsorption efficiency of 83% for EBT and 52% for MB, respectively. Adsorption of MB and EBT on the surface of PPLP₃ membrane is pH dependent. The adsorption of PPLP membrane's follows the pseudo-2nd-order kinetics model and the Langmuir isotherm adsorption model, with R² values of 0.964 and 0.997, respectively. The adsorption mechanism suggested that the pollutants were removed due to the presence of functional groups on PPLP membrane surface. Results show that PPLP₃ has good adsorptive properties for a variety of pollutants from wastewater, therefore, it could be used as a potential adsorbent in the future.

Acknowledgments: The authors acknowledge the support by Sindh Madressatul Islam University for giving the experimental research laboratory facilities.

Conflicts of Interest: There are no conflicts of interest to declare.

| Abbreviation | Details |
|------------------------------------------------------|-----------------------------------------|
| PET | Polyethylene terephthalate |
| PAN | Polyacrylonitrile |
| LDH | Layer double hydroxides |
| PVA | Polyvinyl alcohol |
| EBT | Eriochrome Black T |
| MB | Methylene blue |
| Mw | Molecular weight |
| Mg(NO ₃) ₂ .6H ₂ O | Magnesium nitrate hexahydrate |
| Al(NO ₃) ₃ .9H ₂ O | Aluminum nitrate nonahydrate |
| Na ₂ CO ₃ | Sodium carbonate |
| HCl | Hydrochloric acid |
| NaOH | Sodium hydroxide pellets |
| H ₂ SO ₄ | Sulfuric acid |
| DMF | N, N-Dimethyl formamide |
| TFA | Trifluoro acetic acid |
| DCM | Dichloro methane |
| SEM | Scanning electron microscopy |
| XRD | Xray diffraction |
| EDS | Energy dispersive Xray spectroscopy |
| FTIR | Fourier Transform Infrared Spectroscopy |
| PP | PET-PAN |
| PPLP | PET-PAN-Mg-Al-LDH-PVA |

References

- Abdollahi, E., Heidari, A., Mohammadi, T., Asadi, A. A., & Tofighy, M. A. (2021). Application of Mg-Al LDH nanoparticles to enhance flux, hydrophilicity and antifouling properties of PVDF ultrafiltration membrane: Experimental and modeling studies. *Separation and purification technology*, 257, 117931.
- Ahmad, A., Mohd-Setapar, S. H., Chuong, C. S., Khatoon, A., Wani, W. A., Kumar, R., & Rafatullah, M. (2015). Recent advances in new generation dye removal technologies: novel search for approaches to reprocess wastewater. *RSC advances*, 5(39), 30801-30818.
- Akram, M., Bhutto, S. U. A., Aftab, S., Sindhu, L., Xu, X., & Haider, Z. (2023). Nanocomposites for Removal and Degradation of Organic Pollutants. In *Modern Nanotechnology: Volume I: Environmental Sustainability and Remediation* (pp. 519-558): Springer.
- Al-Sou'od, K. (2012). Adsorption isotherm studies of chromium (VI) from aqueous solutions using Jordanian pottery materials. *Apchee Procedia*, 1, 116-125.
- Aldawsari, A. M., Alshaimi, I., Hassan, H. M., Abdalla, Z. E., Hassan, I., & Berber, M. R. (2021). Tailoring an efficient nanocomposite of activated carbon-layered double hydroxide for elimination of water-soluble dyes. *Journal of Alloys and Compounds*, 857, 157551.
- Alnaqbi, M. A., Samson, J. A., & Greish, Y. E. (2020). Electrospun polystyrene/LDH fibrous membranes for the removal of Cd²⁺ ions. *Journal of Nanomaterials*, 2020, 1-12.
- Anah, L., & Astrini, N. (2017). *Influence of pH on Cr (VI) ions removal from aqueous solutions using carboxymethyl cellulose-based hydrogel as adsorbent*. Paper presented at the IOP Conference Series: Earth and Environmental Science.
- Anandh Babu, M., Hemavathi, S., Kousalyadevi, G., & Shanmuga Priya, S. (2023). Biosorption potential of neem leave powder for the sequestration of arsenic and chromium metal ions.
- Ayandiran, T., Fawole, O., & Dahunsi, S. (2018). Water quality assessment of bitumen polluted Oluwa river, South-Western Nigeria. *Water Resources and Industry*, 19, 13-24.
- Aziz, F. M. A., Surip, S. N., Sekak, K. A., Uyup, M. K. A., Tarawneh, M. a. A., & Lee, S. H. (2021). Evaluation of wetting, structural and thermal properties of electrospun nanofibers at different pineapple leaf fiber/polyethylene terephthalate ratios. *Maderas. Ciencia y tecnología*, 23.
- Baig, N., Matin, A., Faizan, M., Anand, D., Ahmad, I., & Khan, S. A. (2022). Antifouling low-pressure highly permeable single step produced loose nanofiltration polysulfone membrane for efficient Erichrome Black T/divalent salts fractionation. *Journal of Environmental Chemical Engineering*, 10(4), 108166.
- Bakhsh, N., Ahmed, Z., Mahar, R. B., & Khatri, Z. (2021). Development and application of electrospun modified polyvinylidene fluoride (PVDF) nanofibers membrane for biofouling control in membrane bioreactor. *Desalin. Water Treat*, 74-82.
- Bano, Z., Akram, M., Ali, N. Z., Khan, M. U., Wang, F., Li, L., & Xia, M. (2024). Sustainable porous graphene/Co-MOF for the removal of water pollutants: Combined theoretical and experimental studies. *Journal of Water Process Engineering*, 59, 104982.
- Ben Arfi, R., Karoui, S., Mougin, K., & Ghorbal, A. (2019). Cetyltrimethylammonium bromide-treated Phragmites australis powder as novel polymeric adsorbent for hazardous Eriochrome Black T removal from aqueous solutions. *Polymer bulletin*, 76(10), 5077-5102.
- Bensalah, H., Younssi, S. A., Ouammou, M., Gurlo, A., & Bekheet, M. F. (2020). Azo dye adsorption on an industrial waste-transformed hydroxyapatite adsorbent: Kinetics,

- isotherms, mechanism and regeneration studies. *Journal of Environmental Chemical Engineering*, 8(3), 103807.
- Chaukura, N., Murimba, E. C., & Gwenzi, W. (2017). Synthesis, characterisation and methyl orange adsorption capacity of ferric oxide–biochar nano-composites derived from pulp and paper sludge. *Applied Water Science*, 7, 2175-2186.
- Cheng, J., Zhan, C., Wu, J., Cui, Z., Si, J., Wang, Q., . . . Turng, L.-S. (2020). Highly efficient removal of methylene blue dye from an aqueous solution using cellulose acetate nanofibrous membranes modified by polydopamine. *ACS omega*, 5(10), 5389-5400.
- Chiu, H., Lin, J., Cheng, T., & Chou, S. (2011). Fabrication of electrospun polyacrylonitrile ion-exchange membranes for application in lysozym. *Express Polymer Letters*, 5(4).
- da Silva Alves, D. C., Healy, B., Pinto, L. A. d. A., Cadaval Jr, T. R. S. A., & Breslin, C. B. (2021). Recent developments in chitosan-based adsorbents for the removal of pollutants from aqueous environments. *Molecules*, 26(3), 594.
- da Silva, R. J., Mojica-Sánchez, L. C., Gorza, F. D., Pedro, G. C., Maciel, B. G., Ratkovski, G. P., . . . Chávez-Guajardo, A. E. (2021). Kinetics and thermodynamic studies of Methyl Orange removal by polyvinylidene fluoride-PEDOT mats. *Journal of Environmental Sciences*, 100, 62-73.
- Dai, S., Wu, X., Zhang, J., Fu, Y., & Li, W. (2018). Coenzyme A-regulated Pd nanocatalysts for formic acid-mediated reduction of hexavalent chromium. *Chemical Engineering Journal*, 351, 959-966.
- Dhar, L., Hossain, S., Rahman, M. S., Quraishi, S. B., Saha, K., Rahman, F., & Rahman, M. T. (2021). Adsorption mechanism of methylene blue by graphene oxide-shielded Mg–Al-layered double hydroxide from synthetic wastewater. *The Journal of Physical Chemistry A*, 125(4), 954-965.
- Dhar, L., Rahman, M. S., Hossain, S., Quraishi, S. B., Saha, K., Rahman, F., . . . Rahman, M. T. (2022). Mechanistic insights of the adsorption of Eriochrome Black T by the formulated Mg–Al LDH-graphene oxide composite. *Journal of the Iranian Chemical Society*, 19(4), 1319-1328.
- Duman, O., Tunç, S., Polat, T. G., & Bozoğlan, B. K. (2016). Synthesis of magnetic oxidized multiwalled carbon nanotube-κ-carrageenan-Fe₃O₄ nanocomposite adsorbent and its application in cationic Methylene Blue dye adsorption. *Carbohydrate Polymers*, 147, 79-88.
- Ebrahimi, F., Nabavi, S. R., & Omrani, A. (2022). Fabrication of hydrophilic hierarchical PAN/SiO₂ nanofibers by electrospray assisted electrospinning for efficient removal of cationic dyes. *Environmental Technology & Innovation*, 25, 102258.
- Eltaweil, A., Mohamed, H. A., Abd El-Monaem, E. M., & El-Subruiti, G. (2020). Mesoporous magnetic biochar composite for enhanced adsorption of malachite green dye: Characterization, adsorption kinetics, thermodynamics and isotherms. *Advanced Powder Technology*, 31(3), 1253-1263.
- Essa, W. K., Yasin, S. A., Abdullah, A. H., Thalji, M. R., Saeed, I. A., Assiri, M. A., . . . Ali, G. A. (2022). Taguchi L25 (54) Approach for Methylene Blue Removal by Polyethylene Terephthalate Nanofiber-Multi-Walled Carbon Nanotube Composite. *Water*, 14(8), 1242.
- Farooqi, Z. H., Akram, M. W., Begum, R., Wu, W., & Irfan, A. (2021). Inorganic nanoparticles for reduction of hexavalent chromium: Physicochemical aspects. *Journal of hazardous materials*, 402, 123535.

- Guo, R., Guo, W., Pei, H., Wang, B., Guo, X., Liu, N., & Mo, Z. (2021). Polypyrrole deposited electrospun PAN/PEI nanofiber membrane designed for high efficient adsorption of chromium ions (VI) in aqueous solution. *Colloids and Surfaces A: Physicochemical and Engineering Aspects*, 627, 127183.
- Habiba, U., Afifi, A. M., Salleh, A., & Ang, B. C. (2017). Chitosan/(polyvinyl alcohol)/zeolite electrospun composite nanofibrous membrane for adsorption of Cr⁶⁺, Fe³⁺ and Ni²⁺. *Journal of hazardous materials*, 322, 182-194.
- Habiba, U., Lee, J. J. L., Joo, T. C., Ang, B. C., & Afifi, A. M. (2019). Degradation of methyl orange and congo red by using chitosan/polyvinyl alcohol/TiO₂ electrospun nanofibrous membrane. *International Journal of Biological Macromolecules*, 131, 821-827.
- Hartati, S., Zulfi, A., Maulida, P. Y. D., Yudhowijoyo, A., Dioktyanto, M., Saputro, K. E., . . . Rochman, N. T. (2022). Synthesis of electrospun PAN/TiO₂/Ag nanofibers membrane as potential air filtration media with photocatalytic activity. *ACS omega*, 7(12), 10516-10525.
- He, Y., Wu, P., Xiao, W., Li, G., Yi, J., He, Y., . . . Duan, Y. (2019). Efficient removal of Pb (II) from aqueous solution by a novel ion imprinted magnetic biosorbent: Adsorption kinetics and mechanisms. *PloS one*, 14(3), e0213377.
- Hu, W., Wu, X., Jiao, F., Yang, W., & Zhou, Y. (2016). Preparation and characterization of magnetic Fe₃O₄@ sulfonated β-cyclodextrin intercalated layered double hydroxides for methylene blue removal. *Desalination and Water Treatment*, 57(53), 25830-25841.
- Hu, Z.-P., Gao, Z.-M., Liu, X., & Yuan, Z.-Y. (2018). High-surface-area activated red mud for efficient removal of methylene blue from wastewater. *Adsorption Science & Technology*, 36(1-2), 62-79.
- Inam, M. A., Khan, R., Lee, K. H., Akram, M., Ahmed, Z., Lee, K. G., & Wie, Y. M. (2021). Adsorption capacities of iron hydroxide for arsenate and arsenite removal from water by chemical coagulation: Kinetics, thermodynamics and equilibrium Studies. *Molecules*, 26(22), 7046.
- Jeong, C.-B., Lee, Y. H., Park, J. C., Kang, H.-M., Hagiwara, A., & Lee, J.-S. (2019). Effects of metal-polluted seawater on life parameters and the induction of oxidative stress in the marine rotifer *Brachionus koreanus*. *Comparative Biochemistry and Physiology Part C: Toxicology & Pharmacology*, 225, 108576.
- Jia, S., Liang, Y., & Yang, N. (2021). High performance of polyacrylonitrile/[MgAl]-layered double hydroxide composite nanofiber separators for safe lithium-ion batteries. *Solid State Ionics*, 370, 115735.
- Jiang, L., Zhao, Y., & Zhai, J. (2004). A lotus-leaf-like superhydrophobic surface: a porous microsphere/nanofiber composite film prepared by electrohydrodynamics. *Angewandte Chemie-International Edition*, 43(33), 4338-4341.
- Khalid, A., Zubair, M., & Ihsanullah. (2018). A comparative study on the adsorption of Eriochrome Black T dye from aqueous solution on graphene and acid-modified graphene. *Arabian Journal for Science and Engineering*, 43, 2167-2179.
- Khan, M. I., Shanableh, A., Fernandez, J., Lashari, M. H., Shahida, S., Manzoor, S., . . . Elboughdiri, N. (2021). Synthesis of dmea-grafted anion exchange membrane for adsorptive discharge of methyl orange from wastewaters. *Membranes*, 11(3), 166.
- Khorram, M., Mousavi, A., & Mehranbod, N. (2017). Chromium removal using adsorptive membranes composed of electrospun plasma-treated functionalized polyethylene terephthalate (PET) with chitosan. *Journal of Environmental Chemical Engineering*, 5(3), 2366-2377.

- Kishore, K., Hsu, C.-Y., Sridhara, S., Odongo, J. O., Akram, M., Malik, J. A., . . . Manzoor, J. (2023). Fundamentals of Nanotechnology for Environmental Engineering. In *Modern Nanotechnology: Volume 1: Environmental Sustainability and Remediation* (pp. 1-19): Springer.
- Konicki, W., Aleksandrak, M., Moszyński, D., & Mijowska, E. (2017). Adsorption of anionic azo-dyes from aqueous solutions onto graphene oxide: equilibrium, kinetic and thermodynamic studies. *Journal of colloid and interface science*, *496*, 188-200.
- Li, G., Zhao, Y., Lv, M., Shi, Y., & Cao, D. (2013). Super hydrophilic poly (ethylene terephthalate)(PET)/poly (vinyl alcohol)(PVA) composite fibrous mats with improved mechanical properties prepared via electrospinning process. *Colloids and Surfaces A: Physicochemical and Engineering Aspects*, *436*, 417-424.
- Li, L., Luo, C., Li, X., Duan, H., & Wang, X. (2014). Preparation of magnetic ionic liquid/chitosan/graphene oxide composite and application for water treatment. *International Journal of Biological Macromolecules*, *66*, 172-178.
- Li, X., Ding, B., Lin, J., Yu, J., & Sun, G. (2009). Enhanced mechanical properties of superhydrophobic microfibrillar polystyrene mats via polyamide 6 nanofibers. *The Journal of Physical Chemistry C*, *113*(47), 20452-20457.
- Makarov, I. S., Vinogradov, M. I., Golova, L. K., Arkharova, N. A., Shambilova, G. K., Makhatova, V. E., & Naukenov, M. Z. (2022). Design and Fabrication of Membranes Based on PAN Copolymer Obtained from Solutions in N-methylmorpholine-N-oxide. *Polymers*, *14*(14), 2861.
- Mansor, E. S., Ali, H., & Abdel-Karim, A. (2020). Efficient and reusable polyethylene oxide/polyaniline composite membrane for dye adsorption and filtration. *Colloid and Interface Science Communications*, *39*, 100314.
- Manzar, M. S., Waheed, A., Qazi, I. W., Blaisi, N. I., & Ullah, N. (2019). Synthesis of a novel epibromohydrin modified crosslinked polyamine resin for highly efficient removal of methyl orange and eriochrome black T. *Journal of the Taiwan Institute of Chemical Engineers*, *97*, 424-432.
- Mittal, J. (2021). Recent progress in the synthesis of Layered Double Hydroxides and their application for the adsorptive removal of dyes: A review. *Journal of Environmental Management*, *295*, 113017.
- Nasouri, K., Shoushtari, A. M., & Mojtahedi, M. R. M. (2015). Effects of polymer/solvent systems on electrospun polyvinylpyrrolidone nanofiber morphology and diameter. *Polymer Science Series A*, *57*, 747-755.
- Novillo, C., Guaya, D., Avendaño, A. A.-P., Armijos, C., Cortina, J., & Cota, I. (2014). Evaluation of phosphate removal capacity of Mg/Al layered double hydroxides from aqueous solutions. *Fuel*, *138*, 72-79.
- Pan, X., Zhang, M., Liu, H., Ouyang, S., Ding, N., & Zhang, P. (2020). Adsorption behavior and mechanism of acid orange 7 and methylene blue on self-assembled three-dimensional MgAl layered double hydroxide: Experimental and DFT investigation. *Applied Surface Science*, *522*, 146370.
- Pathirana, M. A., Dissanayake, N. S., Wanasekara, N. D., Mahltig, B., & Nandasiri, G. K. (2023). Chitosan-graphene oxide dip-coated polyacrylonitrile-ethylenediamine electrospun nanofiber membrane for removal of the dye stuffs methylene blue and congo red. *Nanomaterials*, *13*(3), 498.

- Picón, D., Vergara-Rubio, A., Estevez-Areco, S., Cervený, S., & Goyanes, S. (2022). Adsorption of Methylene Blue and Tetracycline by Zeolites Immobilized on a PBAT Electrospun Membrane. *Molecules*, 28(1), 81.
- Pirzada, A. M., Ali, I., Mallah, N. B., & Maitlo, G. (2023). Development of Novel PET-PAN Electrospun Nanocomposite Membrane Embedded with Layered Double Hydroxides Hybrid for Efficient Wastewater Treatment. *Polymers*, 15(22), 4388.
- Preethi, G., & Jeyanthi, J. (2023). Biosorption of heavy metals using *Gracilaria edulis* seaweed—batch adsorption, kinetics and thermodynamic studies.
- Qin, Q., Liu, Y., Chen, S. C., Zhai, F. Y., Jing, X. K., & Wang, Y. Z. (2012). Electrospinning fabrication and characterization of poly (vinyl alcohol)/layered double hydroxides composite fibers. *Journal of applied polymer science*, 126(5), 1556-1563.
- Radoor, S., Karayil, J., Jayakumar, A., Parameswaranpillai, J., & Siengchin, S. (2021). Efficient removal of methyl orange from aqueous solution using mesoporous ZSM-5 zeolite: Synthesis, kinetics and isotherm studies. *Colloids and Surfaces A: Physicochemical and Engineering Aspects*, 611, 125852.
- Radoor, S., Karayil, J., Parameswaranpillai, J., & Siengchin, S. (2020). Adsorption study of anionic dye, Eriochrome black T from aqueous medium using polyvinyl alcohol/starch/ZSM-5 zeolite membrane. *Journal of Polymers and the Environment*, 28, 2631-2643.
- Sajid, M., Jillani, S. M. S., Baig, N., & Alhooshani, K. (2022). Layered double hydroxide-modified membranes for water treatment: Recent advances and prospects. *Chemosphere*, 287, 132140.
- Shahverdi, F., Barati, A., & Bayat, M. (2022). Effective Methylene Blue Removal from Aqueous Solutions using PVA/Chitosan Electrospun Nanofiber Modified with CeAlO₃ Nanoparticles. *Journal of Water and Environmental Nanotechnology*, 7(1), 55-68.
- Shakiba, M., Abdouss, M., Mazinani, S., & Kalae, M. R. (2023). Super-hydrophilic electrospun PAN nanofibrous membrane modified with alkaline treatment and ultrasonic-assisted PANI in-situ polymerization for highly efficient gravity-driven oil/water separation. *Separation and purification technology*, 309, 123032.
- Skornyakov, I., & Komar, V. (1998). IR spectra and the structure of plasticized cellulose acetate films. *Journal of applied spectroscopy*, 65, 911-918.
- Swain, S. K., Barik, S., Pradhan, G. C., & Behera, L. (2018). Delamination of Mg-Al layered double hydroxide on starch: change in structural and thermal properties. *Polymer-Plastics Technology and Engineering*, 57(15), 1585-1591.
- Ullah, S., Hashmi, M., Kharaghani, D., Khan, M. Q., Saito, Y., Yamamoto, T., . . . Kim, I. S. (2019). Antibacterial properties of in situ and surface functionalized impregnation of silver sulfadiazine in polyacrylonitrile nanofiber mats. *International journal of nanomedicine*, 2693-2703.
- Wang, N., Zhao, Y., & Jiang, L. (2008). Low-cost, thermoresponsive wettability of surfaces: Poly (N-isopropylacrylamide)/Polystyrene composite films prepared by electrospinning. *Macromolecular Rapid Communications*, 29(6), 485-489.
- Wang, Q., Geng, Y., Lu, X., & Zhang, S. (2015). First-row transition metal-containing ionic liquids as highly active catalysts for the glycolysis of poly (ethylene terephthalate)(PET). *ACS Sustainable Chemistry & Engineering*, 3(2), 340-348.
- Wu, S., Li, K., Shi, W., & Cai, J. (2022). Preparation and performance evaluation of chitosan/polyvinylpyrrolidone/polyvinyl alcohol electrospun nanofiber membrane for

- heavy metal ions and organic pollutants removal. *International Journal of Biological Macromolecules*, 210, 76-84.
- Wu, Y., Luo, H., Wang, H., Wang, C., Zhang, J., & Zhang, Z. (2013). Adsorption of hexavalent chromium from aqueous solutions by graphene modified with cetyltrimethylammonium bromide. *Journal of colloid and interface science*, 394, 183-191.
- Xu, P., Wang, Y., Wang, S., Dai, W., Chen, N., & Li, Q. (2022). Preparation of polyethyleneimine-modified porous polyacrylonitrile electrospun nanofibers for efficient removal of methyl orange. *Journal of Macromolecular Science, Part A*, 59(7), 504-512.
- Yasin, S. A., Sharaf Zeebaree, S. Y., Sharaf Zeebaree, A. Y., Haji Zebari, O. I., & Saeed, I. A. (2021). The efficient removal of methylene blue dye using CuO/PET nanocomposite in aqueous solutions. *Catalysts*, 11(2), 241.
- Zhang, Y., Wu, B., Xu, H., Liu, H., Wang, M., He, Y., & Pan, B. (2016). Nanomaterials-enabled water and wastewater treatment. *NanoImpact*, 3, 22-39.
- Zhao, R., Li, X., Li, Y., Li, Y., Sun, B., Zhang, N., . . . Wang, C. (2017). Functionalized magnetic iron oxide/polyacrylonitrile composite electrospun fibers as effective chromium (VI) adsorbents for water purification. *Journal of colloid and interface science*, 505, 1018-1030.
- Zhu, F., Zheng, Y.-M., Zhang, B.-G., & Dai, Y.-R. (2021). A critical review on the electrospun nanofibrous membranes for the adsorption of heavy metals in water treatment. *Journal of hazardous materials*, 401, 123608.
- Zubair, M., Jarrah, N., Manzar, M. S., Al-Harathi, M., Daud, M., Mu'azu, N. D., & Haladu, S. A. (2017). Adsorption of eriochrome black T from aqueous phase on MgAl-, CoAl- and NiFe-calcined layered double hydroxides: Kinetic, equilibrium and thermodynamic studies. *Journal of Molecular Liquids*, 230, 344-352.

Supplementary information

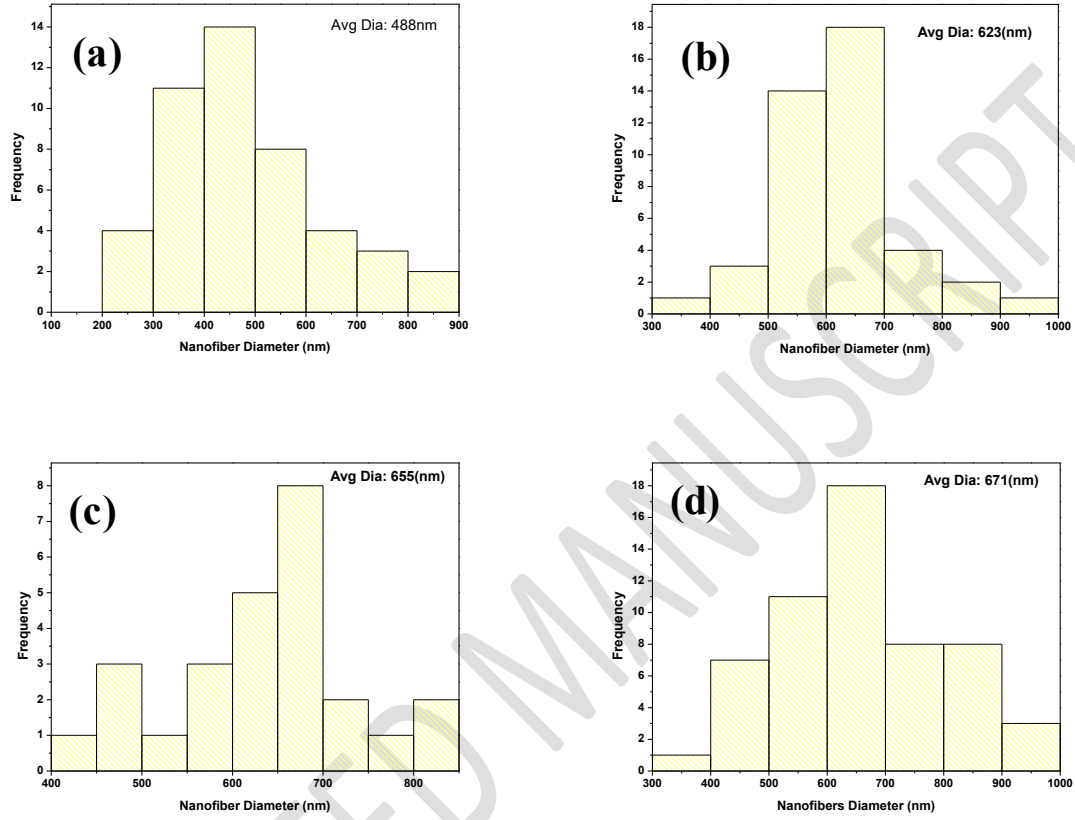


Figure S1. The nanofiber diameter histograms of: (a) PP, (b) PPLP₁, (c) PPLP₂, and (d) PPLP₃ membranes.

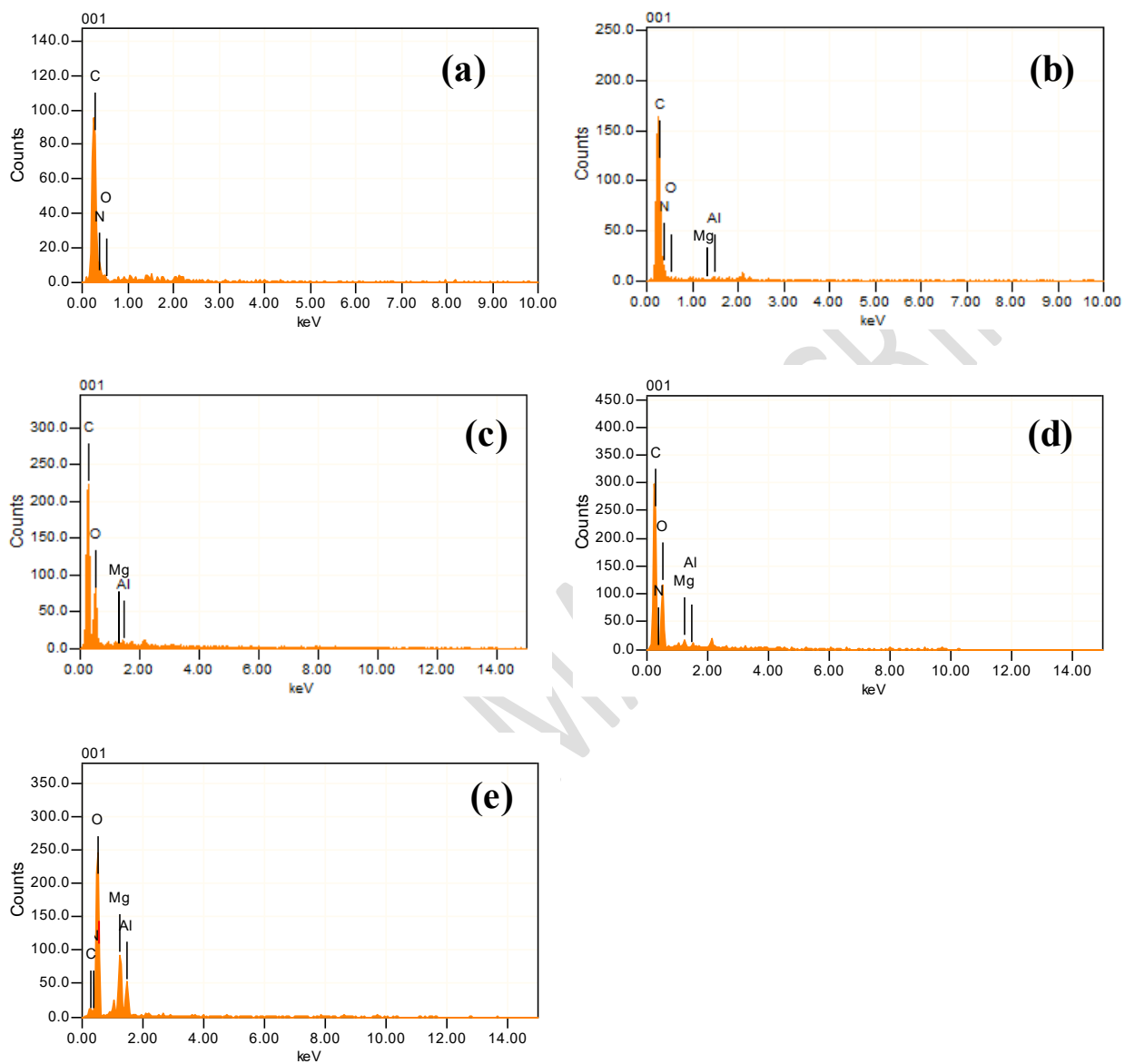


Figure S2. EDS spectrum of: (a) PP, (b) PPLP₁, (c) PPLP₂, (d) PPLP₃, and (e) Mg-Al-LDH.

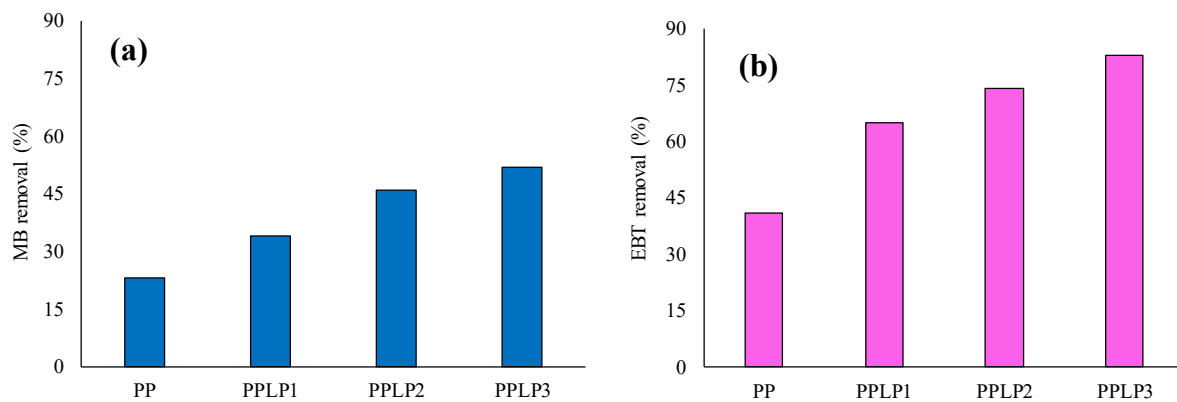


Figure S3. Basic adsorption experiment results for removal of: (a) MB and (b) EBT dyes.

ACCEPTED MANUSCRIPT

Table S1. Basic adsorption experimental conditions for MB and EBT using PP and PPLP membranes.

| Membrane type | Pollutant type | Solution pH | Adsorption time (min) | Concentration (mg.L ⁻¹) | Membrane dosage (mg) | Solution volume (mL) |
|-------------------|----------------|-------------|-----------------------|-------------------------------------|----------------------|----------------------|
| PP | | | | | | |
| PPLP ₁ | MB | 7 | 120 | 10 | 30 | 20 |
| PPLP ₂ | | | | | | |
| PPLP ₃ | | | | | | |
| PP | | | | | | |
| PPLP ₁ | EBT | 3 | 90 | 10 | 30 | 20 |
| PPLP ₂ | | | | | | |
| PPLP ₃ | | | | | | |